



## South Pole Station ozonesondes: variability and trends in the springtime Antarctic ozone hole 1986-2021

Bryan J. Johnson<sup>1</sup>, Patrick Cullis<sup>2,1</sup>, John Booth<sup>†1</sup>, Irina Petropavlovskikh<sup>2,1</sup>,  
Glen McConville<sup>2,1</sup>, Birgit Hassler<sup>3</sup>, Gary A. Morris<sup>1</sup>, Chance Sterling<sup>2,4</sup>, Samuel Oltmans<sup>1</sup>

- 5 <sup>1</sup>Global Monitoring Laboratory Earth System Research Laboratory, NOAA, Boulder, CO, 80305 USA  
<sup>2</sup>Cooperative Institute for Research in Environmental Sciences, University of Colorado, Boulder, CO, USA  
<sup>3</sup>Deutsches Zentrum für Luft & Raumfahrt (DLR), Institut für Physik der Atmosphäre, Oberpfaffenhofen, Germany  
<sup>4</sup>C&D Technologies/Trojan Battery Company, Horsham, PA, 19044 USA  
†deceased

10

*Correspondence to:* Bryan J. Johnson (bryan.johnson@noaa.gov)

- Abstract.** Balloon-borne ozonesondes launched weekly from South Pole station (1986-2021) measure high vertical resolution profiles of ozone and temperature from surface to 30-35 km altitude. The launch frequency is increased in late winter before the onset of rapid stratospheric ozone loss in September. Ozone hole metrics show the yearly total column ozone and 14-21 km column ozone minimum values and September loss rates remain on an upward (less severe) trend since 2001. However, the data series also illustrate interannual variability, especially in the last three years (2019-2021). Here we show additional details of these three years by comparing minimum ozone profiles and the July-December 14-21 km column ozone time series. The 2019 anomalous vortex breakdown showed stratospheric temperatures began warming in early September leading to reduced ozone loss. The minimum total column ozone of 180 Dobson Units (DU) was observed on 24 September. This was followed by two stable and cold polar vortex years in 2020 and 2021 with total column ozone minimums at 104 DU (01 October) and 102 DU (07 October), respectively. These years also showed broad near-zero ozone (saturation loss) regions within the 14-21 km layer by the end of September which persisted into October.
- 20  
25
- Validation of the ozonesonde observations is conducted through the ongoing comparison of total column ozone (TCO) measurements with the South Pole ground-based Dobson spectrophotometer. The ozonesondes show a constant positive offset of  $2 \pm 3\%$  (higher) than the Dobson following a thorough evaluation/homogenization of the ozonesonde record in 2018.

---

### 1 Introduction

30

- In 1986, NOAA began launching weekly balloon-borne ozonesondes at Amundsen-Scott South Pole Station (90°S) measuring high-resolution vertical profiles of ozone and temperature. This same year numerous field projects were deployed to Antarctica (Anderson et al., 1989; Tuck et al., 1989) to investigate the discovery of the springtime Antarctic ozone hole by Farman et al. (1985). Subsequent studies confirmed that the chlorine-catalytic destruction of ozone was enhanced over Antarctica in the presence of winter-time polar stratospheric clouds (PSCs) (Solomon et al., 1986; 1999, McElroy et al., 1986). The following decade of balloon-borne profiles, satellite, and ground-based measurements showed a broad and deepening ozone hole that stabilized in its expansion by the early 2000s (Hofmann et al., 2009). More recently, several analyses of the ongoing ground-based and satellite
- 35



measurements indicate that the ozone hole has been slowly recovering since 2000. The current recovery stage and upward trend in  
springtime ozone has been linked to the decline in the concentration of man-made ozone depleting substances (ODS) due to the  
40 successful implementation of the Montreal Protocol international guidelines phasing out ODS emissions (for list of studies see  
WMO-2018 report). In 2020, the ODS abundance over Antarctica was 25% below the 2001 peak (Montzka et al., 2021). Full  
recovery is predicted to occur by around 2056–2070 when ODS levels return to the 1980-benchmark levels (Newman 2006;  
Dhomse et al., 2018; Amos et al., 2020). However, while long-lived ODS concentrations are steadily declining, the extent of  
chemical ozone loss may be quite different from year-to-year due to meteorological conditions (Newman et al., 2006; Keeble et  
45 al., 2014; de Laat et al., 2017; Tully et al., 2019; Stone et al., 2021).

After polar sunset, the strengthening of circumpolar winds and the development of a potential vorticity gradient forms the  
polar vortex boundary region that isolates stratospheric air over Antarctica (Nash et al., 1996). Near the center of the vortex, over  
the South Pole, ozonesondes measure stratospheric temperatures steadily decreasing during the polar night and remaining well  
below the  $-78^{\circ}\text{C}$  threshold for PSC formation and growth. PSCs provide the surface reaction sites for activating stable chlorine  
50 species into radicals that rapidly destroy ozone after sunlight returns in September (WMO, 2018). However, planetary wave  
disturbances in late winter may weaken or completely break apart the cold and stable Antarctic polar vortex, ending the optimum  
conditions for rapid ozone loss in September (Schoeberl et al., 1989; Newman et al, 2004; Hassler et al., 2011a; Salby et al., 2012;  
Strahan & Douglas, 2016; de Laat et al., 2017; Strahan et al., 2019; Milinevsky et al, 2020). The most extreme atmospheric  
disruptions, resulting in the weakest ozone holes, were observed in 1988, 2002, and 2019 (Stolarski et al., 1990; Hoppel et al.,  
55 2003; Safieddine et al., 2020; Wargan et al., 2020). 1986 was also a year with a considerably weaker polar vortex.

The South Pole ozonesondes play a key role in monitoring ozone and temperature during all phases of the ozone hole and are  
especially critical after the Antarctic sunset when darkness limits most stratospheric observations. Several indices and indicators  
have been presented in past analyses of the Antarctic ozonesonde records by Hofmann et al, (1997, 2009); Solomon et al., (2005,  
2016); and Hassler et al., (2011). This paper is a review of the South Pole ozonesonde observations beginning with an overview in  
60 Sect. 2 of the electrochemical concentration (ECC) ozonesonde and recent homogenization of the South Pole data record by  
Sterling et al. (2018). Section 3 shows a comparison of ozone and temperature profiles during the last 3 years when the early polar  
vortex breakup and weak ozone hole in September 2019 was followed by severe ozone loss in 2020 and 2021 when cold vortex  
conditions persisted into October (Kramarova et al., 2021). Section 4 shows the updated 36-year homogenized ozone time series  
and ozone hole metrics focusing on the 14–21 km layer column ozone minimums and linear ozone loss rates during September. In  
65 addition, we update ozone mixing ratio loss rates at selected pressure levels from the analysis by Hassler et al., (2011a) in which  
the 89 hPa layer was found to be the optimum for detecting recovery in September ozone loss. Section 5 illustrates the extent of  
saturation loss observed each year during the minimum ozone period from 26 September to 15 October. The near-zero ozone layers  
were variable and narrowing after 2008, but were near maximum extent again in 2020 and 2021. The summary is given in Sect. 6.

## 2 ECC ozonesonde overview

70 The basic design of the electrochemical concentration cell (ECC) ozonesonde has remained relatively unchanged during the 36-  
year South Pole record (Komhyr, 1967). A Teflon piston pump bubbles ambient air into a sensor cell chamber with a platinum  
gauze electrode submerged in 3 cc of dilute, buffered potassium iodide (KI) solution. The ozone/iodide reaction in the ECC cell  
generates the electrical signal proportional to ozone. Since about the mid-1990s, the ECC sonde manufacturers have improved the  
sensor cell design and the purity of the platinum electrodes, thus reducing the limit of detection (LOD) to a partial pressure of 0.07



75 millipascals ( $< 0.03$  microamps). This equates to an LOD of 10 ppbv at 70 hectopascals (hPa). The Styrofoam box houses and  
insulates the ozonesonde pump and sensor. The weather radiosonde, attached to the outside of the box, measures and transmits  
meteorological and ozone data to the ground-based receiving equipment during ascent to the balloon-burst altitude of about 34 km.  
Consistent burst altitudes are maintained during the dark, cold months at South Pole by switching from standard rubber weather  
balloons to 18k-19k volume polyethylene film balloons during the first week of April then returning to rubber balloons by mid-  
80 October.

## 2.1 Data Homogenization

Each ECC ozonesonde profile represents a new instrument, used only once, thus, ozonesonde trends may show an offset or sudden  
bias rather than a slow drift in the data record when a new ozonesonde design or standard operating procedure change occurs  
(Johnson, et al., 2002; Smit et al., 2007; Tarasick et al., 2016; Van Malderen et al., 2016). The ozonesonde model and standard  
85 operating procedures (SOPs) at South Pole have not changed since 2006. However, prior to 2006, several dual and triple  
ozonesondes were flown to compare new ozonesonde models or adjustments made in the SOP in order to determine ad hoc  
corrections to account for these changes. A thorough review and homogenization of the ozonesonde record was completed by  
Sterling et al. (2018) following the homogenization guidelines from the Assessments of Standard Operating Procedures (ASOPOS  
GAW/WMO report # 268, 2021). The guidelines are based on the Jülich World Ozonesonde Calibration Center Ozone  
90 Intercomparison Experiments (JOSIE). The JOSIE environmental simulation chamber experiments are the global reference for  
evaluation of new ozonesonde designs and SOPs and the foundation for improving long-term vertical ozone trends determined by  
ozonesondes with a goal to reduce uncertainty to  $\pm 5\%$  throughout the profile (Smit et al., 2007; Thompson et al., 2019)

Additional verification of ozonesonde measurements at South Pole station is conducted through the ongoing comparison of  
total column ozone (TCO) with the NOAA ground-based Dobson spectrophotometer which measures direct sun (DS) TCO over  
95 South Pole station from 20 October to 20 February (Komhyr et al., 1997). The Dobson Spectrophotometer global network is  
recognized as the long-term stable reference for balloon-borne observations and for identifying drifts in satellite platforms  
(McPeters & Komhyr, 1991; Bodeker et al., 2005; Thompson et al., 2017). Figure 1 shows the ozonesonde TCO after  
homogenization with a constant  $2 \pm 3\%$  offset, slightly higher than the DS Dobson observations. The ozonesonde TCO includes a  
residual value to account for estimated ozone above the balloon burst altitude by extrapolating a constant mixing ratio (CMR)  
100 from the balloon burst pressure ( $\sim 20$  to 7 hPa) to zero pressure. While the satellite SBUV global climatological residual tables from  
McPeters et al. (1997) are the current standard for determining ozonesonde residuals for most locations on the globe, the CMR  
extrapolation is more suitable over South Pole during the polar night and low sun angle months when satellite and ground-based  
optical measurements are limited.

## 2.2 Temperature Profile Validation

105 Sterling et al. (2018) discusses the details in the transition from three different radiosonde models at South Pole from VIZ (1986-  
1991) to Vaisala RS-80 (1991-2014) and the current GPS-enabled InterMet (Imet) radiosondes (2015-2021). The Imet  
measurements added winds and geometric altitude to the South Pole profile data.

The ozonesonde radiosonde temperatures were not adjusted in the homogenization of the data record. However, temperature  
accuracy for each flight is validated by comparing with a second radiosonde flown by the Met Service at South Pole. For nearly a



110 decade, the Met Service meteorological radiosondes (using Vaisala RS92 and Vaisala RS-41 models) were “piggy-backed” on  
board the NOAA ozonesonde package. This comparison is important during the dark and coldest winter months when NOAA  
switches to the cold-resistant polyethylene balloons to record the full profile from surface to 30-34 km (rubber balloons typically  
fail/burst at 14-15 km over South Pole under these extreme conditions). The comparisons between the Vaisala radiosonde models  
(RS80 and RS92) during 2012-2013 flights show almost no difference in stratospheric temperature measurement during the  
115 summer months and only a slight 0.2°C difference in winter. The Imet radiosonde measures slightly higher temperatures, by about  
0.5°C, than the Vaisala RS41, primarily during the summer months.

### 3 South Pole Ozonesonde Profiles: 2019-2021

Balloon-borne ozonesondes provide a unique overview of the yearly ozone hole over South Pole by comparing the profiles  
measured during winter before depletion begins, and after when the minimum ozone is typically observed between 26 September  
120 to 15 October. Figure 2 shows the 2019-2021 ozone (upper panel) and temperature (lower panel) profiles representing the ozone  
holes of these three years. The winter profiles (blue) are an average of the 6-8 profiles measured from 15 June to 15 August, when  
the stratospheric temperatures range between -85 to -95 °C and total column ozone (TCO) averages  $263 \pm 17$  DU. The wintertime  
profiles are similar each year and typically don't provide any insight into how the polar vortex conditions and ozone depletion will  
unfold when rapid depletion begins by 01 September. However, ozonesonde measurements around the last two weeks of August  
125 may show signs of ozone depletion above 21 km over South Pole from air parcels that have been illuminated near the polar vortex  
boundaries where  $\text{Cl}_2$  photolysis begins (Schoeberl et al., 1992; Lee et al., 2001; Hassler, et al, 2011a; Strahan et al., 2019). The  
springtime minimum TCO profiles (red) average of  $114 \pm 15$  Dobson Units (DU) represents a 55-65% ozone loss when compared  
to the wintertime profile. The 2019 minimum TCO of 180 DU was observed on 24 September, the 2nd highest minimum in the  
36-year South Pole record. This was the 3rd season when the polar vortex was dramatically disrupted leading to an early September  
130 warming and meridional mixing of ozone-rich air into the polar region from the mid-latitude stratosphere (Wargen et al., 2020;  
Safieddine, et al., 2020). Table 1 lists the other two years (1988 and 2002) when similar events occurred. The table also includes  
the date intervals when data was excluded in our long-term median calculations since these extremes in ozone and temperatures  
were not representative of typical chemical ozone hole losses.

135 Table 1. Years when an early disruption of the polar vortex was observed over South Pole and the corresponding period when the  
profile data was excluded from the ozonesonde median and percentile climatology.

Year	Dates excluded	Event
1988	11 Aug – 01 Dec	Early vortex weakening in August
2002	22 Sep – 15 Dec	Sudden stratospheric warming / split vortex (Allen et al., 2003)
2019	05 Sep – 20 Dec	Sudden stratospheric warming /vortex shift (Safieddine et al., 2020)

140 The stable and cold polar vortex conditions in 2020 and 2021 led to severe ozone holes over South Pole with minimum total  
column ozone measurements of 104 DU on 01 October and 102 DU on 07 October, respectively. The profiles in Fig. 2 show nearly  
complete destruction of ozone within the 14-21 km vertical layer observed during those two years. The record low total column  
ozone profile in 2006 (92 DU) on 09 October, shown as the dotted line in Fig. 2, had a vertical extent of near-zero ozone (ozone  
loss saturation) from 14 to 21 km. Thereafter, the 14-21 km layer became the baseline for loss rate metrics (Sect. 4) for tracking



potential recovery (Hofmann et al., 2009). The term “near-zero ozone” from here on will represent stratospheric ozone partial  
145 pressure measurements that fall below 0.2 millipascals (three times the LOD). The next section shows all of the observations of  
the 14-21 km column ozone during 2019-2021 from July-December to illustrate the temporal evolution and variability of the ozone  
hole.

### 3.1 South Pole Ozonesondes 14-21 km time series: 2019-2021

Figure 3 shows the July-December time series of 14-21 km column ozone and temperature in 2019, 2020, and 2021 compared to  
150 the 1986-2021 climatological median with 30-70th /10-90th percentiles in gray shading. The median and percentile values were  
calculated using a sliding time series bin that is gradually reduced from  $\pm 14$ -days in July to a  $\pm 3$ -day bin during the month of  
September when more frequent ozonesonde launches track the rapidly decreasing ozone column. The slope of the median 14-21  
km column ozone (black line) decreases linearly during September at a rate of  $-3.5$  DU/day, this metric is computed for each  
individual year and presented in Section 4 to show the ozone loss rate trend. After 01 November the ozone and temperature  
155 percentiles broaden significantly due to variable dates when the Antarctic polar vortex fully dissipates (Karpetchko et al., 2005;  
Bodeker et al., 2005).

The stratospheric warming event in 2019 included a large-scale shift of the polar vortex towards the tip of South America  
(Safieddine, et al., 2020), away from the typical position centered near the South Pole. Figure 3 shows the anomalous high ozone  
and temperature breakout in September 2019 over South Pole. The 08 September temperature profile showed the first sign of this  
160 weakening vortex with an abrupt increase of more than  $10^\circ$  C in the 14-21 km layer. However, the column ozone within the 14-21  
km layer remained close to the median line until 20 September when the strong depletion period ended and ozone values leveled  
off in the 45-50 DU range. Then on 10 October, dropped to the minimum for the year at 44 DU when the polar vortex briefly  
centered back over the continent and South Pole station.

The opposite polar vortex conditions were observed in 2020 and 2021 when cold temperatures and column ozone tracked  
165 well below the median near the lower edge of the 10-90th percentile line from September through December in Fig. 3. Both years  
showed severe loss in the 14-21 km column with a minimum of 2 DU (2020) and 3 DU (2021), both occurring on 01 October,  
followed by a slow recovery. The year 2020 was the slowest recovery on record at South Pole based on the daily Dobson  
Spectrophotometer TCO direct-sun measurements which resumed by mid-October at 109 DU, then remained below the 220 DU  
ozone hole threshold (Stolarksi et al., 1990) until 12 December when the Dobson spectrophotometer measured 236 DU.

### 170 4 Ozonesonde Metrics: Altitude Intervals: 1986-2021

Table 2 lists the altitude layer metrics analyzed in this study that are focusing on ozone loss during September and the minimum  
by early October. While the lowest ozone is a key metric of ozone hole severity each year, many recovery indices focus on the  
September observations when the highest sensitivity and correlation with decreasing ODSs may be ascribed (Solomon et al. 2016;  
de Latt et al., 2017; Pazmiño et al., 2018; Strahan et al., 2019). The South Pole ozonesonde metrics here focus on the 14-21 km  
175 layer and include two additional metrics showing an update of the mixing ratio loss rate profiles at selected pressure levels from  
Hassler et al. (2011a) and a metric showing the yearly vertical extent of layers with near-zero ozone.

Table 2. Altitude Layers and Metrics updated for 1986-2021 ozonesonde record at South Pole.



Altitude Layer	Metric – plotted data
14-21 km	Column ozone minimums (DU) & September loss rates (DU/day)
Pressure: 119-33 hPa	September mixing ratio loss rate profiles (ppmv/day)
10-24 km – curtain plot	Near-zero ozone (mPa) layers during minimum period (Sep26-Oct15)
<i>Dobson Units (DU)</i>	<i>Mixing Ratio – parts per million by volume (ppmv)</i>
<i>Millipascals (mPa)</i>	<i>Hectopascals (hPa)</i>

180 Figure 4a-b shows an overview of the 36-year time series of selected values of 14-21 km integrated column ozone representing the three stages of the ozone hole over South Pole. The upper panel (Fig. 4a) shows ozone observed before depletion begins and after (spring minimum ozone) and also includes a middle time series when an ozonesonde is launched each year on September 15th to track the progress of ozone depletion (Hofmann et al., 2009). The winter average 14-21 km column ozone (15 June - 15 August) has been relatively constant at  $130 \pm 10$  DU. However, when September ozone depletion begins the downward trend becomes more evident in the 15 September series after 1986, followed by recovery in 2000/2001. The slope of the trend lines shown in Fig. 4a were computed by the LOTUS model (Long-term Ozone Trends and Uncertainties – described in the SPARC/IO3C/GAW report, 2019). The LOTUS regression was run for this data series without seasonal components.

185 The spring minimum series bottomed out at near-zero ozone in the 14-21 km layer from 1993-2001 followed by an upward trend. While both the 15 September and spring minimum series show year-to-year variability, the three anomalous polar vortex break up years (red dots) stand out as peaks in the minimum series while the 15 September observations show almost no signal. This is due to the location of South Pole situated far from the polar vortex edge where there is greater dynamical influence in ozone observations (Hassler et al., 2011b). In addition, the 14-21 km is below the altitude ( $\sim >24$  km) region where more dynamic variability first appears as higher ozone and temperature layers over South Pole as the vortex begins breaking up.

190 The lower panel (Fig. 4b) shows the difference between the three series in Fig. 4a to illustrate the 14-21 km layer ozone total loss each year and the loss that occurred before and after 15 September. From 1991-2000, there was an increasing trend in the 14-21 km column ozone loss during the first half of September (blue line in Fig 4-b) reaching a peak of 100 DU loss in 2000. This was followed by a downward trend with significant variability, until reaching a relatively stable 60-65 DU after 2014. The loss during the second half of September depends on the amount of ozone remaining after 15 September and meteorological conditions governing the stability of the polar vortex. An early vortex weakening or break up may result in transport and mixing of high ozone air masses with the depleted ozone thus reducing or ending loss before the end of September. The year 2021 shows the second highest overall loss on record at 133 DU. This year began at a slower than average pace of ozone loss with 59 DU of loss by 15 September but followed with a record loss of 74 DU for the second half of September with only 3 DU remaining in the 14-21 km layer on 01 October.

#### 4.1 September column ozone loss rates: 14-21 km

205 Figure 5 shows the yearly September ozone column (14-21 km) loss rates from the ozonesondes launched every 2-4 days during late August until mid-October. The selection of the start and end day for the  $\sim 30$ -day loss period are adjusted forward or backward by  $\pm 3$  days to obtain the best linear fit to the observations (see method description in Hassler et al., 2011a). In late September, near the minimum date, the linear depletion data point selection ends when either a sharp increase in ozone is observed or, in severe depletion years, drops to near-zero or shifts to a non-linear loss rate when approaching saturation ozone loss. The selected values between the start and end points are used to determine the loss rate slope and uncertainty by a linear regression model. The 36-



year time series shows that the 14-21 km column ozone loss rate has improved from a minimum of -3.8 DU/day during 2002-2007 to -3 DU/day in 2016-2021, which can be an early indicator of recovery over South Pole noted by Hofmann et al. (1997, 2009). The sudden stratospheric warming year in 2002 (red dot) showed rapid ozone loss but within a shortened time period ending on September 22, when the first sign of the sudden stratospheric warming (increase in ozone and temperature) began to show at altitudes above 21 km. The following ozonesonde profile on September 25 in 2002 showed substantial ozone increases throughout the 15 to 32 km layer resulting in a record high TCO of 397 DU. In 2019, the loss rate calculation period was also shortened to just two weeks before the linear ozone decline ended on September 15th. The loss rate data point for 2019 is included in Figure 5 with high uncertainty.

#### 4.2 September ozone mixing ratio loss rates: 119-33 hectopascals

Hassler et al. (2011a) analyzed vertical profiles of ozone mixing ratio loss rates in twenty layers from 200 to 10 hPa showing that peak loss rates occurred near the 48 and 33 hPa layers. The lower variability at 89 hPa was found to be optimal to identify the earliest signs of ozone recovery, estimated to occur around 2021. Figure 6 shows the September ozone mixing ratio loss rates (ppmv/day) for five selected layers from 119 hPa (13.6 km) to 33 hPa (20.6 km). Following the analysis method by Hassler et al. (2011a), the ozone mixing ratios during September (~Day 235-270) are grouped in 5-year intervals to reduce the influence of prevailing phases of the quasi-biennial oscillation (QBO) and other dynamical processes. Figure 6 shows that overall loss rates peaked during 2001-2005. All the selected pressure layers showed decreases in loss rates by 2016-2020. The 89 hPa loss rate showed improvement (29% decrease) with the lowest variability as predicted in the earlier assessment. The highest altitude layer at 33 hPa level showed a substantial 50% decline from the 2001-2005 peak loss rate.

Figure 7 shows the 1986-2021 temperature time series for the five pressure levels during the month of September and before sunrise from 15 July to 15 August when stratospheric temperatures remain cold (-90 to -94 °C) and stable. No temperature trends are apparent in any of the time series. However, 2021 stands out as the coldest September observed at all pressure levels. In addition, Figure 7 shows that the stable vortex in 2021 remained very cold with almost no temperature difference between winter and September at pressure levels of 119, 89, and 67 hPa and just 2 to 3°C warmer at 48 and 33 hPa. This was similar to the record low ozone year in 2006, but the 2006 temperatures were not as cold as 2021. The highest temperatures occurred in 2002 after the sudden stratospheric warming on 22 September when the 30-50 degree increase in temperature observed from 100-20 hPa sent the September temperature average off scale in Figure 7.

#### 5 Saturation ozone loss: near-zero ozone layers

The near complete destruction of stratospheric ozone (saturation loss) within the 14-21 km layer is a feature of the Antarctica ozone hole that is observed in detail by high-resolution ozonesondes. Near the end of September, as the linear decrease in ozone begins to slow, other nonlinear depletion reactions complete the pathway to near-zero ozone (Grooß et al., 2011; Kuttippurath et al., 2018; Muller et al., 2018). A reduction in the vertical extent of the near-zero ozone layers will be an important indicator of recovery showing when decreasing equivalent effective stratospheric chlorine (EESC) is no longer the excess component in the reactions that destroy ozone (Kuttippurath et al., 2018).

The vertical extent of near-zero ozone layers observed over South Pole is shown in Figure 8 as a curtain plot of dark to light gray shaded bars showing only the lowest partial pressure minimums from 0 to 0.7 millipascals (mPa). These values represent a



95-99% loss compared to the 14-16 mPa values observed during the winter before ozone depletion begins (see Fig. 2). The near-zero ozone values for each year are selected from the lowest partial pressure ozone out of all 7-9 profiles flown during the minimum ozone hole period (26 September – 15 October). All values greater than 0.7 mPa are not included in order to highlight the lowest ozone region. The three early vortex breakup years, listed in Table 2, are shown as light red bars when ozone minimums were > 4-5 mPa.

Figure 9 shows the average temperature curtain plot during the minimum ozone period. The PSC threshold temperature of  $-78^{\circ}\text{C}$  is selected as the break point between cold (blue) and warm (red) temperature scales. Together, Figs 8 and 9 show the coincidence of years with cold temperatures and low ozone. The recurring year-to-year severe depletion from 1991-2001 shows that the upper boundary of the near complete ozone loss layer was extending to higher altitudes each year, eventually peaking at 21 km. Hofmann et al., (1997) and Hoppel et al., (2003) noted that a reversal of ozone loss in the upper altitudes would be an indication of recovery. Figure 8 shows that after the record low in 2006, the near-zero ozone vertical extent appeared to be narrowing and becoming irregular. Then in 2020 and 2021 ozonesondes observed the optimum cold polar vortex conditions in September to late October along with extensive near-zero ozone within 13.5 to 20.5 km altitude. However, the 7 km near-zero ozone layer was not observed in a single profile as it was in the record low ozone profile in 2006. For example, in 2021 the near-zero ozone layer was initially observed at 15-20.5 km on October 1, and from 13.5-17.5 km on 21 October.

Zero ozone extending below 14 km is less common during the ozone minimum period over South Pole. However, volcanic eruption plumes may transport sulphate aerosol southward into the polar stratosphere reducing ozone concentrations through surface reaction processes (Hofmann & Solomon, 1989). For example, there was significant depletion from 12-14 km in 1992-1994 after the major eruption of Mount Pinatubo in 1991 (Hofmann et al., 1993; Deshler et al., 1996). The Calbuco eruption in 2015 also led to an increase in ozone loss below about 14 km (100 hPa) at South Pole (Stone et al., 2017). The recent Hunga Tonga - Hunga Ha'apai volcanic plume reached altitudes up to 30 km after the eruption on 15 January 2022 in the SW Pacific Ocean (Carr et al., 2022). The possible impact of volcanic aerosols on stratospheric ozone within the Antarctic polar vortex in 2022 and 2023 will be monitored by ozonesondes.

## 6 Summary

The South Pole station ozonesondes provide essential year-round high-resolution ozone and temperature profiles tracking all phases of the Antarctic yearly ozone hole near the core of the polar vortex, monitoring both the winter development of the vortex, the conditions that lead up to ozone depletion, and looking precisely in the region where the ozone loss is taking place. The 36-year ozonesonde record has been reviewed, homogenized, and validated by comparing total column ozone with the South Pole Dobson spectrophotometer direct-sun total column ozone measurements. Ozonesondes show a constant positive bias of  $2 \pm 3\%$ .

The 2019, 2020, and 2021 South Pole ozonesonde measurements showed the greatest year-to-year variability in ozone hole conditions ever observed in the South Pole long-term record. The anomalous polar vortex warming in 2019 disrupted ozone depletion in early September resulting in the second weakest ozone hole on record, but the following two years saw cold and persistent vortex conditions with total ozone column minimums among the 10th lowest in the 36-year record. The record low ozone year in 2006 represents the South Pole baseline for metrics tracking ozone recovery listed below compared to the minimum values in the 2019-2021 years:

Year	Minimum Total Column	Minimum 14-21 km	14-21 km September Loss Rate
• 36-year:	114±15 DU	8±5 DU	-2.4 / -3.9 min DU/day





285	• 2006:	92 (09 Oct)	1 (09 Oct)	-3.9
	• 2019:	180 (24 Sep)	44 (10 Oct)	depletion ended 15 September
	• 2020:	104 (01 Oct)	2 (01 Oct)	-3.0
	• 2021:	102 (07 Oct)	3 (01 Oct)	-3.0

The updated time series (1986-2021) of 14-21 km column ozone and September loss rates (Dobson Units/day) show an upward trend (decrease in ozone minimums and loss rate) after 2001. Also, the column ozone losses during the first half of September appears to have slowed.

The September mixing ratio loss rates at selected pressure levels in 5-year periods all showed improvements by 2016-2020 compared to the peak loss period in 2001-2005. The ozone loss at 33 hPa showed the greatest improvement with a 49% reduction in loss rate. The optimum pressure level (89 hPa) for detecting recovery showed a 26% reduction with the lowest variability as predicted by Hassler et al. (2011a). However, the return of severe ozone destruction appeared in 2020 and 2021 with the near 7-km vertical extent of saturated ozone loss (near-zero ozone) observed within the 13.5 to 20.5 km altitude layer during the first three weeks of October under persistent cold and stable vortex conditions.

The long uninterrupted 36-year South Pole ozonesonde record and future balloon-borne measurements will provide unique and vital data for ozone hole recovery analyses. The year-round observations will also be beneficial for observing anomalies in the ozone layer from meteorological events disrupting the polar vortex, and identifying layers where volcanic aerosols influence ozone depletion.

**Data availability** Datasets in this study can be obtained through NOAA ozone archive <https://gml.noaa.gov/aftp/data/ozwv/>. NDACC from <https://www.ndaccdemo.org/stations/south-pole-antarctica>

**Competing interests:** The authors declare that they have no conflict of interest

#### 310 **Special issue statement:**

This article is part of the special issue “Atmospheric ozone and related species in the early 2020s: latest results and trends (ACP/AMT inter-journal SI)”. It is a result of the 2021 Quadrennial Ozone Symposium (QOS) held online on 3–9 October 2021.

#### **Acknowledgements**

The authors are indebted to the many personnel who conducted the balloon flights over the 36-year period at the South Pole spending full year assignments in extreme cold and high-altitude conditions. Without their dedicated service to the US National Oceanic and Atmospheric Administration this work would have been impossible. We thank Allen Jordan, the NOAA/GML/OZWV Division programmer/electronics engineer, for the ongoing development of the extremely valuable balloon tracking telemetry and data analysis SkySonde software. Birgit Hassler was supported by the Helmholtz Society project “Advanced Earth System Model Evaluation for CMIP” (EVal4CMIP). We also acknowledge the logistics support in Antarctica provided by the National Science Foundation, Office of Polar Programs. Finally, we sadly note the passing of coauthor Johan Booth in June 2021, several months after being diagnosed with an aggressive form of cancer. In fifteen years working with NOAA, Johan spent eleven of those wintering at South Pole consistently carrying out meticulous ozonesonde and Dobson observations at South Pole Station.

#### 325 **References**



- Allen, D. R., Bevilacqua, R. M., Nedoluha, G. E., Randall, C. E., and Manney, G. L.: Unusual stratospheric transport and mixing during the 2002 Antarctic winter, *Geophys. Res. Lett.*, 30, 10.1029/2003gl017117, 2003.
- 330 Amos, M., Young, P. J., Hosking, J. S., Lamarque, J. F., Abraham, N. L., Akiyoshi, H., Archibald, A. T., Bekki, S., Deushi, M., Jockel, P., Kinnison, D., Kirner, O., Kunze, M., Marchand, M., Plummer, D. A., Saint-Martin, D., Sudo, K., Tilmes, S., and Yamashita, Y.: Projecting ozone hole recovery using an ensemble of chemistry-climate models weighted by model performance and independence, *Atmos. Chem. Phys.*, 20, 9961-9977, 10.5194/acp-20-9961-2020, 2020.
- 335 Anderson, J. G., Brune, W. H., and Proffitt, M. H.: Ozone destruction by chlorine radicals within the Antarctic vortex - the spatial and temporal evolution of ClO-O<sub>3</sub> anticorrelation based on insitu ER-2 data, *J. Geophys. Res.-Atmos.*, 94, 11465-11479, 10.1029/JD094iD09p11465, 1989.
- 340 Bodeker, G. E., Shiona, H., and Eskes, H.: Indicators of Antarctic ozone depletion, *Atmos. Chem. Phys.*, 5, 2603-2615, 10.5194/acp-5-2603-2005, 2005.
- Carr, J. L., Horvath, A., Wu, D. L., and Friberg, M. D.: Stereo plume height and motion retrievals for the record-setting Hunga Tonga-Hunga Ha'apai eruption of 15 January 2022, *Geophys. Res. Lett.*, 49, 10.1029/2022gl098131, 2022.
- 345 de Laat A. T. J., M. Weele, R. J. A, Onset of stratospheric ozone recovery in the Antarctic ozone hole in assimilated daily total ozone columns, *Journal of Geophysical Research: Atmospheres*, 122, 21, 11,880-11,899, 10.1002/2016JD025723, 2017.
- Deshler, T., Johnson, B. J., Hofmann, D. J., and Nardi, B.: Correlations between ozone loss and volcanic aerosol at altitudes below 14 km over McMurdo Station, Antarctica, *Geophys. Res. Lett.*, 23, 2931-2934, 10.1029/96gl02819, 1996.
- 350 Dhomse, S. S., Kinnison, D., Chipperfield, M. P., Salawitch, R. J., Cionni, I., Hegglin, M. I., Abraham, N. L., Akiyoshi, H., Archibald, A. T., Bednarz, E. M., Bekki, S., Braesicke, P., Butchart, N., Dameris, M., Deushi, M., Frith, S., Hardiman, S. C., Hassler, B., Horowitz, L. W., Hu, R.-M., Jöckel, P., Josse, B., Kirner, O., Kremser, S., Langematz, U., Lewis, J., Marchand, M., Lin, M., Mancini, E., Marécal, V., Michou, M., Morgenstern, O., O'Connor, F. M., Oman, L., Pitari, G., Plummer, D. A., Pyle, J. A., Revell, L. E., Rozanov, E., Schofield, R., Stenke, A., Stone, K., Sudo, K., Tilmes, S., Visionsi, D., Yamashita, Y., and Zeng, G.: Estimates of ozone return dates from Chemistry-Climate Model Initiative simulations, *Atmos. Chem. Phys.*, 18, 8409-8438, <https://doi.org/10.5194/acp-18-8409-2018>, 2018.
- 355 Farman, J. C., Gardiner, B. G., and Shanklin, J. D.: Large losses of total ozone in Antarctica reveal seasonal ClO<sub>x</sub>/NO<sub>x</sub> interaction, *Nature*, 315, 207-210, 10.1038/315207a0, 1985.
- 360 Grooß, J. U., Brautusch, K., Pommrich, R., Solomon, S., and Müller, R.: Stratospheric ozone chemistry in the Antarctic: what determines the lowest ozone values reached and their recovery?, *Atmos. Chem. Phys.*, 11, 12217-12226, 10.5194/acp-11-12217-2011, 2011.
- 365 Hassler, B., Daniel, J. S., Johnson, B. J., Solomon, S., and Oltmans, S. J.: An assessment of changing ozone loss rates at South Pole: Twenty-five years of ozonesonde measurements, *J. Geophys. Res.-Atmos.*, 116, 10.1029/2011jd016353, 2011a.
- 370 Hassler, B., Bodeker, G. E., Solomon, S., and Young, P. J.: Changes in the polar vortex: Effects on Antarctic total ozone observations at various stations, *Geophysical Research Letters*, 38, 10.1029/2010gl045542, 2011b.
- Hofmann, D. J. and Solomon, S.: Ozone destruction through heterogeneous chemistry following the eruption of El Chichon, *J. Geophys. Res.-Atmos.*, 94, 5029-5041, 10.1029/JD094iD04p05029, 1989.
- 375 Hofmann, D. J. and Oltmans, S. J.: Anomalous Antarctic ozone during 1992 - evidence for Pinatubo volcanic aerosol effects, *J. Geophys. Res.-Atmos.*, 98, 18555-18561, 10.1029/93jd02092, 1993.
- Hofmann, D. J., Oltmans, S. J., Harris, J. M., Johnson, B. J., and Lathrop, J. A.: Ten years of ozonesonde measurements at the south pole: Implications for recovery of springtime Antarctic ozone, *J. Geophys. Res.-Atmos.*, 102, 8931-8943, 10.1029/96jd03749, 1997.
- 380 Hofmann, D. J., Johnson, B. J., and Oltmans, S. J.: Twenty-two years of ozonesonde measurements at the South Pole, *Int. J. Remote. Sens.*, 30, 3995-4008, 10.1080/01431160902821932, 2009.



- 385 Hoppel, K., Bevilacqua, R., Allen, D., Nedoluha, G., and Randall, C.: POAM III observations of the anomalous 2002 Antarctic ozone hole, *Geophys. Res. Lett.*, 30, 10.1029/2003gl016899, 2003.
- Johnson, B. J., Oltmans, S. J., Vomel, H., Smit, H. G. J., Deshler, T., and Kroger, C.: Electrochemical concentration cell (ECC) ozonesonde pump efficiency measurements and tests on the sensitivity to ozone of buffered and unbuffered ECC sensor cathode solutions, *J. Geophys. Res.-Atmos.*, 107, 10.1029/2001jd000557, 2002.
- 390 Keeble, J., Braesicke, P., Abraham, N. L., Roscoe, H. K., and Pyle, J. A.: The impact of polar stratospheric ozone loss on Southern Hemisphere stratospheric circulation and climate, *Atmos. Chem. Phys.*, 14, 13705-13717, 10.5194/acp-14-13705-2014, 2014.
- 395 Komhyr, W. D.: Nonreactive gas sampling pump, *Rev. Sci. Instrum.*, 38, 981-&, 10.1063/1.1720949, 1967.
- Komhyr, W. D., Reinsel, G. C., Evans, R. D., Quincy, D. M., Grass, R. D., and Leonard, R. K.: Total ozone trends at sixteen NOAA/CMDL and cooperative Dobson spectrophotometer observatories during 1979-1996, *Geophys. Res. Lett.*, 24, 3225-3228, 400 10.1029/97gl03313, 1997.
- Kramarova, N. A., Newman P. A., Nash E. R., Strahan, S.E. Strahan, Johnson, B., Pitts, M., Santee, M.L., Petropavlovskikh, I., Coy, L., and De Laat, J.: "2021 Antarctic ozone hole [in "State of the Climate in 2021"]." *Bull. Amer. Meteor. Soc.* 103 (8): S26-S29, doi.org/10.1175/BAMS-D-22-00104.1, 2021.
- 405 ]
- Kuttippurath, J., Kumar, P., Nair, P. J., and Pandey, P. C.: Emergence of ozone recovery evidenced by reduction in the occurrence of Antarctic ozone loss saturation, *Npj Climate and Atmospheric Science*, 1, 10.1038/s41612-018-0052-6, 2018.
- 410 McElroy, M. B., Salawitch, R. J., Wofsy, S. C., and Logan, J. A.: Reductions of Antarctic ozone due to synergistic interactions of chlorine and bromine, *Nature*, 321, 759-762, 10.1038/321759a0, 1986.
- McPeters, R. D. and Komhyr, W. D.: Long-term changes in the total ozone mapping spectrometer relative to world primary standard Dobson spectrometer-83, *J. Geophys. Res.-Atmos.*, 96, 2987-2993, 10.1029/90jd02091, 1991.
- 415 McPeters, R. D., Labow, G. J., and Johnson, B. J.: A satellite-derived ozone climatology for balloonsonde estimation of total column ozone, *J. Geophys. Res.-Atmos.*, 102, 8875-8885, 10.1029/96jd02977, 1997.
- 420 Milinevsky, G., Evtushevsky, O., Klekociuk, A., Wang, Y., Grytsai, A., Shulga, V., and Ivaniha, O.: Early indications of anomalous behaviour in the 2019 spring ozone hole over Antarctica, *Int. J. Remote Sens.*, 41, 7530-7540, 10.1080/2150704x.2020.1763497, 2020.
- Montzka, S.A., Dutton, G.S., Butler, J.H., The NOAA Ozone Depleting Gas Index: Guiding Recovery of the Ozone Layer. NOAA Earth System Research Laboratory. <https://gml.noaa.gov/hats/odgi.html> (2021).
- 425 Muller, R., Grooss, J. U., Zafar, A. M., Robrecht, S., and Lehmann, R.: The maintenance of elevated active chlorine levels in the Antarctic lower stratosphere through HCl null cycles, *Atmos. Chem. Phys.*, 18, 2985-2997, 10.5194/acp-18-2985-2018, 2018.
- 430 Nash, E. R., Newman, P. A., Rosenfield, J. E., and Schoeberl, M. R.: An objective determination of the polar vortex using Ertel's potential vorticity, *J. Geophys. Res.-Atmos.*, 101, 9471-9478, 10.1029/96jd00066, 1996.
- Newman, P. A., Nash, E. R., Kawa, S. R., Montzka, S. A., and Schauffler, S. M.: When will the Antarctic ozone hole recover?, *Geophys. Res. Lett.*, 33, 10.1029/2005gl025232, 2006.
- 435 Pazmiño, A., Godin-Beekmann, S., Hauchecorne, A., Claud, C., Khaykin, S., Goutail, F., Wolfram, E., Salvador J., and Quel, E. (2017). Multiple symptoms of total ozone recovery inside the Antarctic vortex during Austral spring. *Atmos. Chem. Phys.* 18, 7557-7572. doi:10.5194/acp-18-7557-20182018
- 440 Salby, M. L., Titova, E. A., and Deschamps, L.: Changes of the Antarctic ozone hole: Controlling mechanisms, seasonal predictability, and evolution, *J. Geophys. Res.-Atmos.*, 117, 10.1029/2011jd016285, 2012.



- 445 Safieddine, S., Bouillon, M., Paracho, A. C., Jumelet, J., Tence, F., Pazmino, A., Goutail, F., Wespes, C., Bekki, S., Boynard, A., Hadji-Lazaro, J., Coheur, P. F., Hurtmans, D., and Clerbaux, C.: Antarctic ozone enhancement during the 2019 sudden stratospheric warming event, *Geophys. Res. Lett.*, 47, 10.1029/2020gl087810, 2020.
- Schoeberl, M. R., Stolarski, R. S., and Krueger, A. J.: The 1988 Antarctic ozone depletion - comparison with previous year depletions, *Geophys. Res. Lett.*, 16, 377-380, 10.1029/GL016i005p00377, 1989.
- 450 Smit, H. G. J., Straeter, W., Johnson, B. J., Oltmans, S. J., Davies, J., Tarasick, D. W., Hoegger, B., Stubi, R., Schmidlin, F. J., Northam, T., Thompson, A. M., Witte, J. C., Boyd, I., and Posny, F.: Assessment of the performance of ECC-ozonesondes under quasi-flight conditions in the environmental simulation chamber: Insights from the Juelich Ozone Sonde Intercomparison Experiment (JOSIE), *J. Geophys. Res.-Atmos.*, 112, 10.1029/2006jd007308, 2007.
- 455 Solomon, S., Garcia, R. R., Rowland, F. S., and Wuebbles, D. J.: On the depletion of Antarctic ozone, *Nature*, 321, 755-758, 10.1038/321755a0, 1986.
- Solomon, S.: Stratospheric ozone depletion: A review of concepts and history, *Rev. Geophys.*, 37, 275-316, 10.1029/1999rg900008, 1999.
- 460 Solomon, S., Portmann, R. W., Sasaki, T., Hofmann, D. J., and Thompson, D. W. J.: Four decades of ozonesonde measurements over Antarctica, *J. Geophys. Res.-Atmos.*, 110, 10.1029/2005jd005917, 2005.
- Solomon, S., Ivy, D. J., Kinnison, D., Mills, M. J., Neely, R. R., and Schmidt, A.: Emergence of healing in the Antarctic ozone layer, *Science*, 353, 269-274, 10.1126/science.aae0061, 2016.
- 470 SPARC/IO3C/GAW, 2019: SPARC/IO3C/GAW Report on Long-term Ozone Trends and Uncertainties in the Stratosphere. I. Petropavlovskikh, S. Godin-Beekmann, D. Hubert, R. Damadeo, B. Hassler, V. Sofieva (Eds.), SPARC Report No. 9, GAW Report No. 241, WCRP-17/2018, doi: 10.17874/f899e57a20b, available at [www.sparc-climate.org/publications/sparc-reports](http://www.sparc-climate.org/publications/sparc-reports).
- Sterling, C. W., Johnson, B. J., Oltmans, S. J., Smit, H. G. J., Jordan, A. F., Cullis, P. D., Hall, E. G., Thompson, A. M., and Witte, J. C.: Homogenizing and estimating the uncertainty in NOAA's long-term vertical ozone profile records measured with the electrochemical concentration cell ozonesonde, *Atmos. Meas. Tech.*, 11, 3661-3687, <https://doi.org/10.5194/amt-11-3661-2018>, 2018.
- 475 Stolarski, R. S., Schoeberl, M. R., Newman, P. A., McPeters, R. D., and Krueger, A. J.: The 1989 Antarctic ozone hole as observed by TOMS, *Geophys. Res. Lett.*, 17, 1267-1270, <https://doi.org/10.1029/GL017i009p01267>, 1990.
- 480 Stone, K. A., Solomon, S., Kinnison, D. E., Pitts, M. C., Poole, L. R., Mills, M. J., Schmidt, A., Neely, R. R., Ivy, D., Schwartz, M. J., Vernier, J. P., Johnson, B. J., Tully, M. B., Klekociuk, A. R., Konig-Langlo, G., and Hagiya, S.: Observing the impact of Calbuco volcanic aerosols on south polar ozone depletion in 2015, *J. Geophys. Res.-Atmos.*, 122, 11862-11879, 10.1002/2017jd026987, 2017.
- 485 Stone, K. A., Solomon, S., Kinnison, D. E., and Mills, M. J.: On recent large Antarctic ozone holes and ozone recovery metrics, *Geophys. Res. Lett.*, 48, 10.1029/2021gl095232, 2021.
- Strahan, S. E., Douglass, A. R., and Steenrod, S. D.: Chemical and dynamical impacts of stratospheric sudden warmings on Arctic ozone variability, *J. Geophys. Res.-Atmos.*, 121, 11836-11851, 10.1002/2016jd025128, 2016.
- 490 Strahan, S. E., Douglass, A. R., and Damon, M. R.: Why do Antarctic ozone recovery trends vary?, *J. Geophys. Res.-Atmos.*, 124, 8837-8850, 10.1029/2019jd030996, 2019.
- 495 Tarasick, D. W., Davies, J., Smit, H. G. J., and Oltmans, S. J.: A re-evaluated Canadian ozonesonde record: measurements of the vertical distribution of ozone over Canada from 1966 to 2013, *Atmos. Meas. Tech.*, 9, 195-214, 10.5194/amt-9-195-2016, 2016.
- 500 Thompson, A. M., Witte, J. C., Sterling, C., Jordan, A., Johnson, B. J., Oltmans, S. J., Fujiwara, M., Vomel, H., Allaart, M., Piders, A., Coetzee, G. J. R., Posny, F., Corrales, E., Andres Diaz, J., Felix, C., Komala, N., Nga, L., Nguyen, H. T. A., Maata, M., Mani, F., Zainal, Z., Ogino, S.-y., Paredes, F., Penha, T. L. B., da Silva, F. R., Sallons-Mitro, S., Selkirk, H. B., Schmidlin, F. J., Stubi, R., and Thiongo, K.: First reprocessing of Southern Hemisphere Additional Ozonesondes (SHADOZ) ozone profiles (1998-2016): 2. comparisons with satellites and ground-based instruments, *J. Geophys. Res.-Atmos.*, 122, 13000-13025, 10.1002/2017jd027406, 2017.



- 505 Thompson, A. M., Smit, H. G. J., Witte, J. C., Stauffer, R. M., Johnson, B. J., Morris, G., von der Gathen, P., Van Malderen, R., Davies, J., PETERS, A., Allaart, M., Posny, F., Kivi, R., Cullis, P., Nguyen Thi Hoang, A., Corrales, E., Machinini, T., da Silva, F. R., Paiman, G., Thiong'o, K., Zainal, Z., Brothers, G. B., Wolff, K. R., Nakano, T., Stubi, R., Romanens, G., Coetzee, G. J. R., Diaz, J. A., Mitro, S., Mohamad, M., and Ogino, S.-Y.: Ozone-sonde quality assurance the JOSIE-SHADOZ (2017) Experience, *B. Am. Meteorol. Soc.*, 100, 155-171, 10.1175/bams-d-17-0311.1, 2019.
- 510 Tuck, A. F., Watson, R. T., Condon, E. P., Margitan, J. J., and Toon, O. B.: The planning and execution of ER-2 and DC-8 aircraft flights over Antarctica, August and September 1987, *J. Geophys. Res.-Atmos.*, 94, 11181-11222, 10.1029/JD094iD09p11181, 1989.
- 515 Tully, M.B., Krummel, P.B., and Klekociuk, A.R.: Trends in Antarctic ozone hole metrics 2001–17, *Journal of Southern Hemisphere Earth Systems Science*, 69, doi:10.1071/es19020, 2019.
- Van Malderen, R., Allaart, M. A. F., De Backer, H., Smit, H. G. J., and De Muer, D.: On instrumental errors and related correction strategies of ozone sondes: possible effect on calculated ozone trends for the nearby sites Uccle and De Bilt, *Atmos. Meas. Tech.*, 9, 3793-3816, 10.5194/amt-9-3793-2016, 2016.
- 520 Wargan, K., Weir, B., Manney, G. L., Cohn, S. E., and Livesey, N. J.: The Anomalous 2019 Antarctic Ozone Hole in the GEOS Constituent Data Assimilation System With MLS Observations, *J. Geophys. Res.-Atmos.*, 125, 10.1029/2020jd033335, 2020.
- 525 World Meteorological Organization: Scientific Assessment of Ozone Depletion: 2006, Global Ozone Research and Monitoring Project – Report No. 50, Geneva, Switzerland, 572 pp., 2007
- World Meteorological Organization: Scientific Assessment of Ozone Depletion: 2018, Global Ozone Research and Monitoring Project – Report No. 58, Geneva, Switzerland, 572 pp., 2018
- 530
- 535

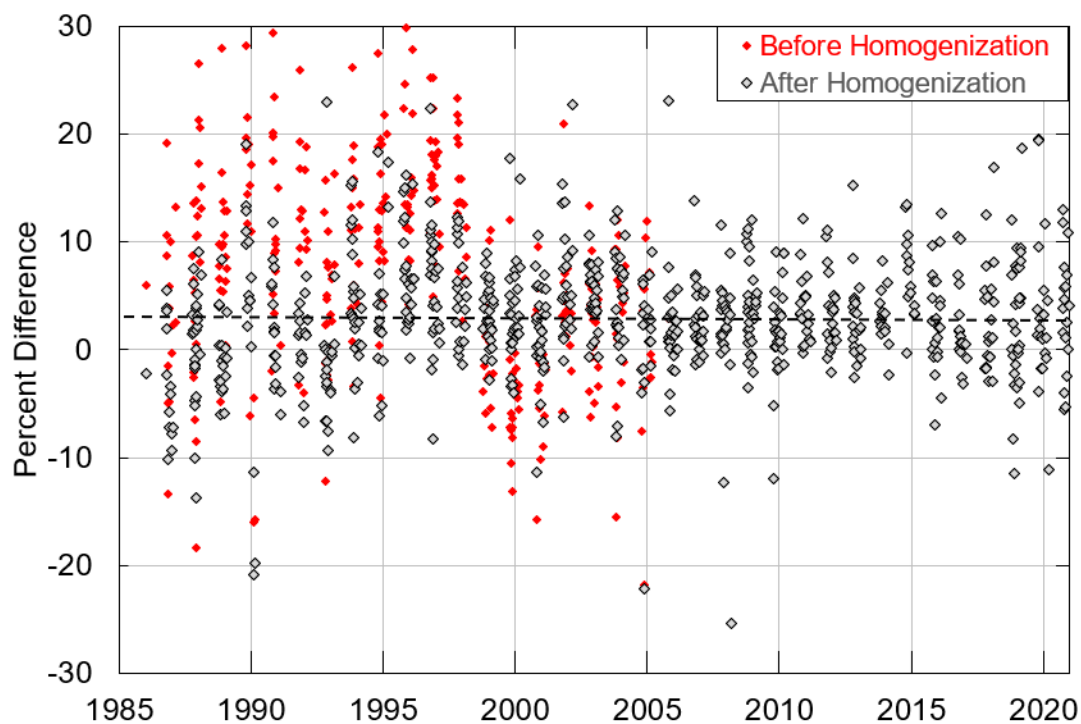
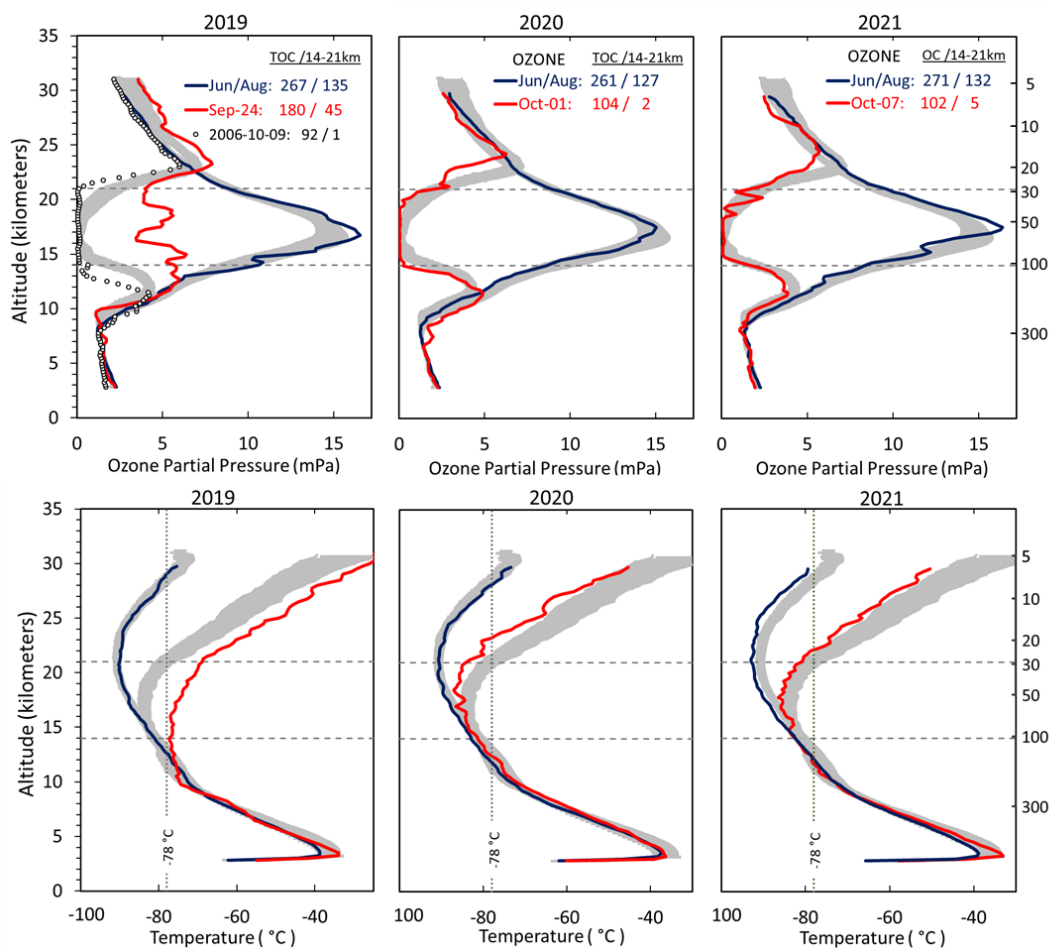


**Figure 1.** Total column ozone comparison of ozonesondes and the Dobson spectrophotometer direct sun measurements. The red diamonds represent the percent differences before the homogenization of 1986-2006 ozonesonde data.



545

**Figure 2.** Selected ozonesonde profiles from 2019-2021 representing the ozone hole severity over South Pole by comparing the average winter profile (before depletion begins/blue line) to the minimum profile (red). The gray-shaded region represents the 1986-2018 median 30-70th percentile during the two periods. The record low of 92 DU total column ozone measured in 2006 is shown as a dotted line in the 2019 graph. The horizontal dashed lines outline the primary depletion region from 14-21 km layer. The temperature graphs mark the  $-78\text{ }^{\circ}\text{C}$  PSC threshold.

555

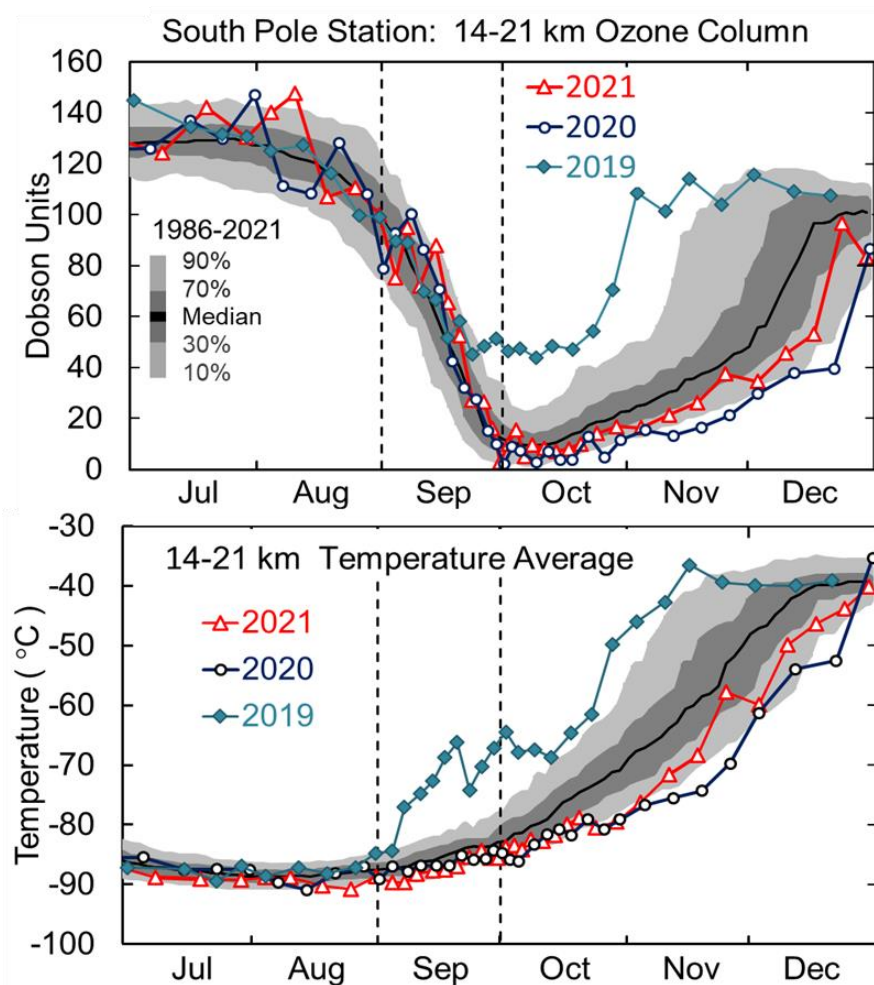
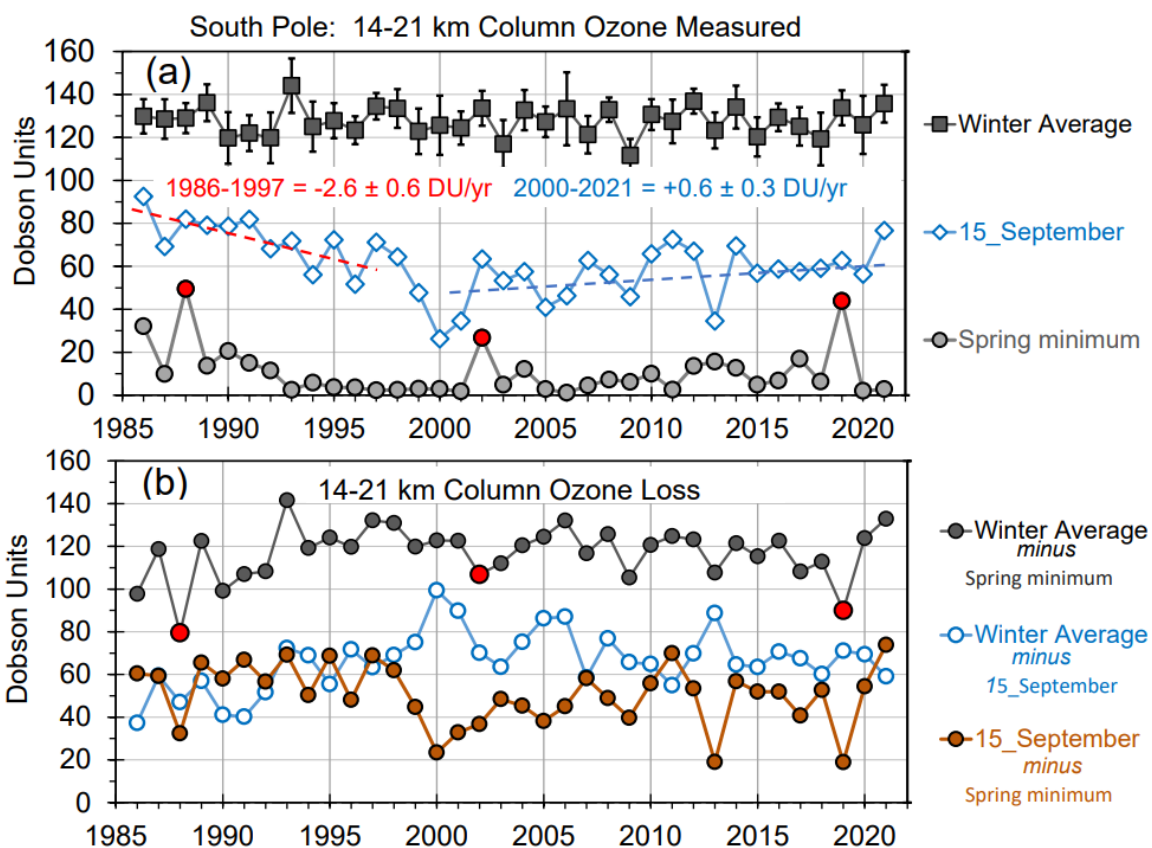


**Figure 3.** South Pole 14-21 km column ozone in Dobson Units (DU) and average temperature tracking the progression of the ozone depletion and recovery from July to December by comparing the long term median with individual years from 2019 to 2021.



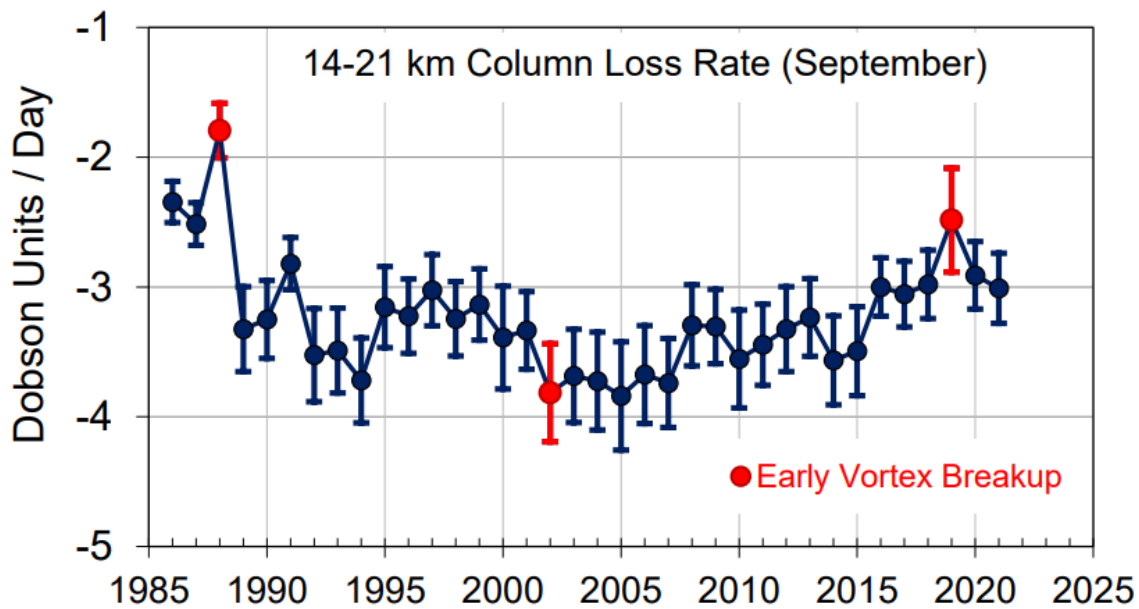
565



570

**Figure 4.** (a) The 1986-2021 measurements of 14-21 km column ozone over South Pole in Dobson Units (DU) during three stages of the ozone hole. The dashed linear lines show trends determined by the LOTUS model regression for the 15 September measurements before and after 2000/2001. (b) The lower panel shows the difference between the three time series in the upper panel to illustrate maximum column ozone loss, the loss during the first half (blue line) and second half (orange line) of the depletion period during September.

575



580

**Figure 5.** Column ozone 14-21 km loss rates [DU/day] during September. The three anomalous vortex years are shown as red dots.



585

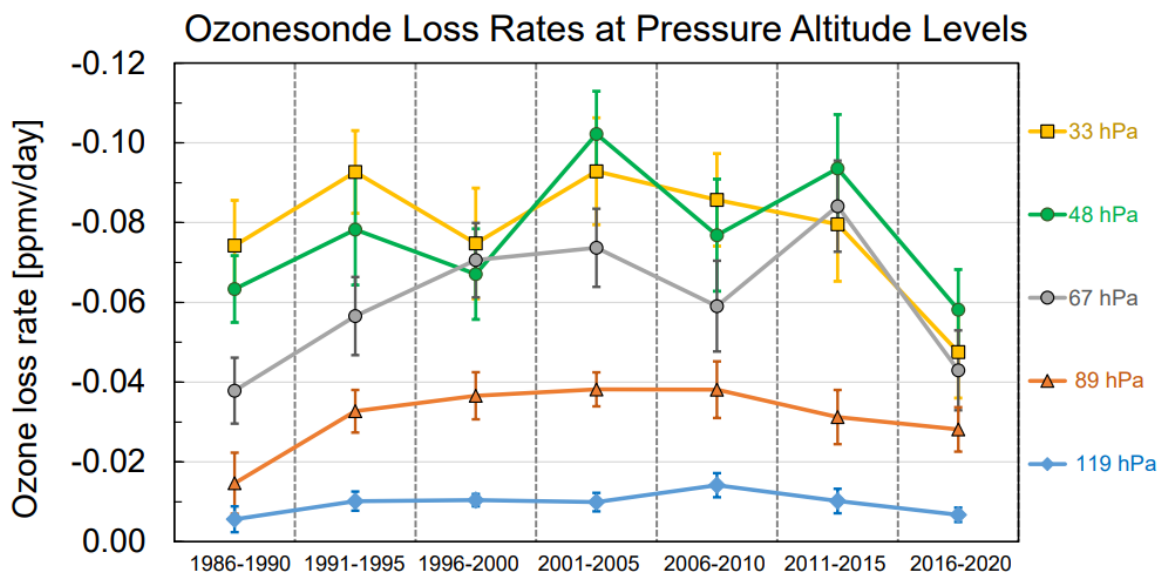
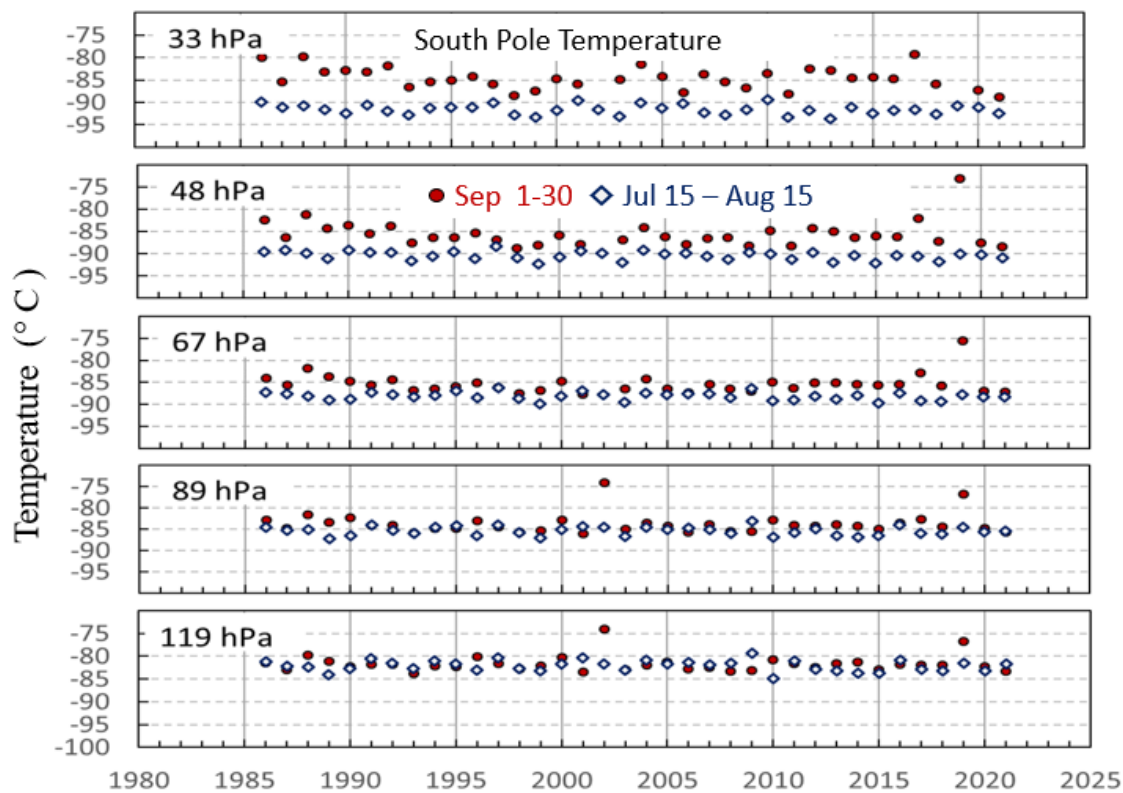
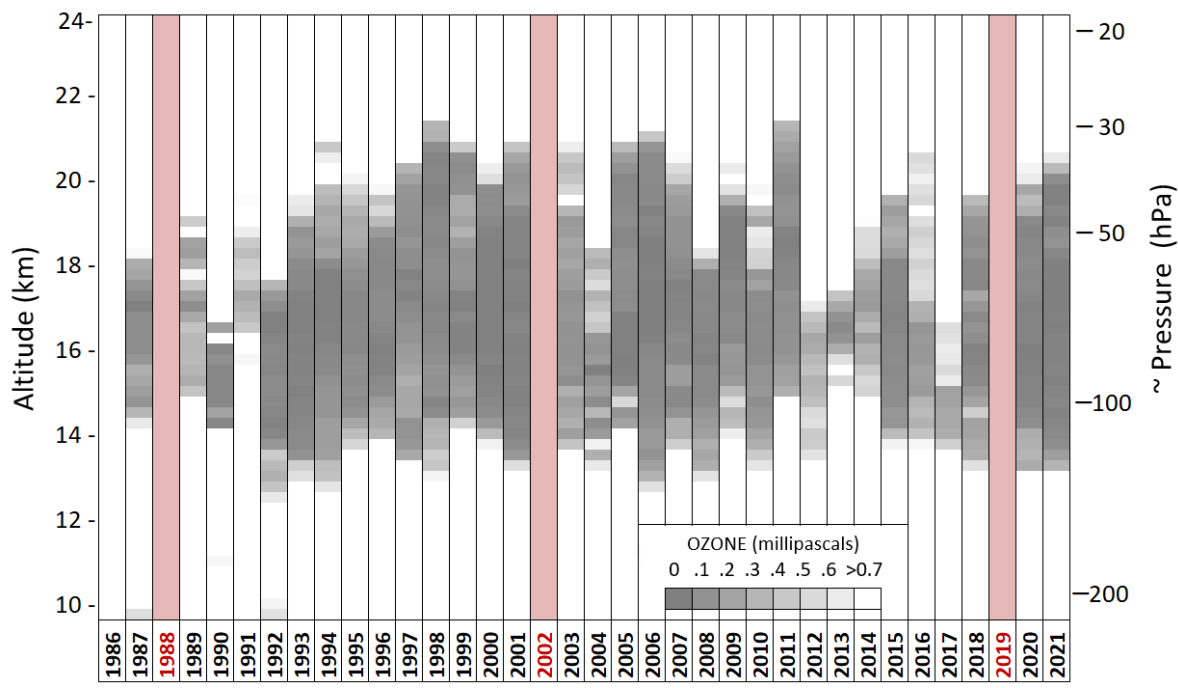


**Figure 6.** September loss rates [ppmv/day] at selected pressure levels within the primary depletion layer from 119 hPa (13.6 km) to 33 hPa (20.6 km).

590



595 **Figure 7.** Average 30-day temperatures during July 15 to August 15 (blue diamonds) September 1-30 (red circles) at the selected pressure levels within the primary depletion layer from 119 hPa (13.6 km) to 33 hPa (20.6 km).



600

**Figure 8.** South Pole 10-24 km curtain plots of the lowest observed ozone partial pressure during the yearly ozone hole minimum period from 24 September to 15 October.

605

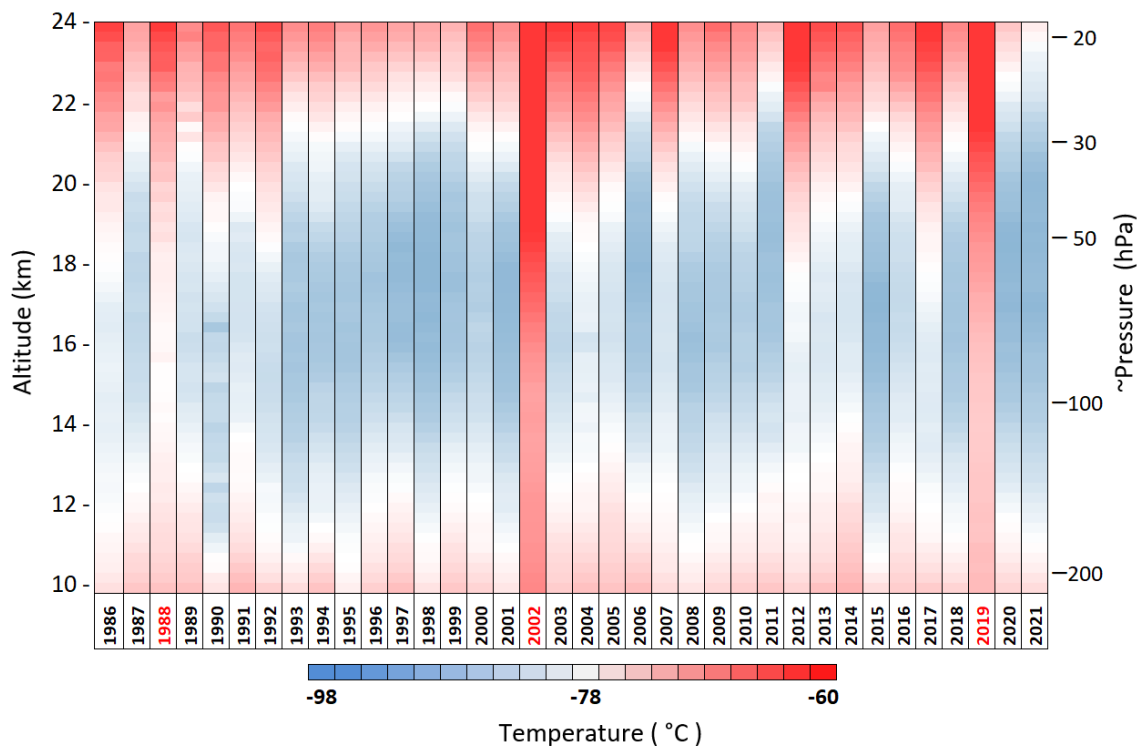


**Figure 9.** The average temperature during 24 September to 15 October (ozone hole minimum period over South Pole Station).

610

615